

Synchrotron-radiation study of the two-leg spin-ladder $(\text{VO})_2\text{P}_2\text{O}_7$ at 120 K

Sandra Geupel,^{a*} Katrin Pilz,^a Sander van Smaalen,^a Frank Büllesfeld,^b Andrei Prokofiev^b and Wolf Assmus^b

^aLaboratory of Crystallography, University of Bayreuth, D-95440 Bayreuth, Germany, and ^bInstitute of Physics, University of Frankfurt, D-60054 Frankfurt am Main, Germany

Correspondence e-mail: sandra.geupel@uni-bayreuth.de

Received 8 October 2001

Accepted 16 October 2001

Online 14 December 2001

The crystal structure of the ambient-pressure phase of vanadyl pyrophosphate, $(\text{VO})_2\text{P}_2\text{O}_7$, has been precisely determined at 120 K from synchrotron X-ray diffraction data measured on a high-quality single crystal. The structure refinement unambiguously establishes the orthorhombic space group $Pca2_1$ as the true crystallographic symmetry. Moreover, it improves the accuracy of previously published atomic coordinates by one order of magnitude, and provides reliable anisotropic displacement parameters for all atoms. Along the a axis, the structure consists of infinite two-leg ladders of vanadyl cations, $(\text{VO})^{2+}$, which are separated by pyrophosphate anions, $(\text{P}_2\text{O}_7)^{4-}$. Parallel to the c axis, the unit cell comprises two alternating crystallographically inequivalent chains of edge-sharing VO_5 square pyramids bridged by PO_4 double tetrahedra. No structural phase transition has been observed in the temperature range between 300 and 120 K.

Comment

Oxovanadium phosphates constitute a family of compounds with a versatile crystallochemistry that results in an intricate magnetochemistry. This diversity is due to the accessibility of several oxidation states of vanadium, the ability of phosphate and vanadium polyhedra to form a large variety of complex network structures, and the involvement of phosphate groups in the spin transfer between V ions. Vanadyl pyrophosphate, $(\text{VO})_2\text{P}_2\text{O}_7$, has been extensively studied by chemists, because this compound is known to be a very efficient catalyst for selective oxidation of n -butane to maleic anhydride (Centi *et al.*, 1988). This process is of considerable industrial importance, as it is presently the only (heterogeneously catalyzed) alkane oxidation performed on a large scale. Recently, $(\text{VO})_2\text{P}_2\text{O}_7$ has attracted much attention by solid-state physicists due to its low-dimensional magnetic properties. It represents a quantum magnetic spin system of V^{4+} ions ($3d^1$ configuration, spin $S = \frac{1}{2}$), whose antiferromagnetic super-

exchange interactions give rise to a non-magnetic singlet ground state accompanied by a singlet–triplet energy gap (Barnes *et al.*, 1993; Eccleston *et al.*, 1994). From a crystallographic point of view, $(\text{VO})_2\text{P}_2\text{O}_7$ has been widely considered to be a prototype of a two-leg spin-ladder system. $S = \frac{1}{2}$ spin ladders are of interest as an intermediate stage between one-dimensional spin chains and two-dimensional spin lattices, and it has been proposed that hole-doped spin ladders may exhibit superconductivity (Dagotto *et al.*, 1992; Dagotto & Rice, 1996). The magnetism of $(\text{VO})_2\text{P}_2\text{O}_7$ has been interpreted in a number of ways, which have been reviewed in detail by Johnston *et al.* (2001). Initially, magnetic susceptibility measurements and inelastic neutron scattering data were discussed in terms of a two-leg spin-ladder model (Barnes & Riera, 1994; Eccleston *et al.*, 1994) and an alternating spin-chain model (Johnston *et al.*, 1987; Barnes & Riera, 1994). Subsequent inelastic neutron scattering studies revealed that the magnetic properties are dominated by alternating spin chains, because the dispersion of magnetic excitations was found to be inconsistent with a spin ladder (Garrett, Nagler, Barnes & Sales, 1997; Garrett, Nagler, Tennant *et al.*, 1997). Recently, high-field magnetization measurements, and NMR and Raman scattering studies proved the co-existence of two magnetic subsystems associated with two different spin-gap energies (Kikuchi *et al.*, 1999; Yamauchi *et al.*, 1999; Kuhlmann *et al.*, 2000).

Several studies of the crystal structure of $(\text{VO})_2\text{P}_2\text{O}_7$ at room temperature have been published. Initial diffraction experiments with X-rays and electrons suggested orthorhombic symmetry with space group $Pcam$ or $Pca2_1$ (Gorbunova & Linde, 1979; Bordes & Courtine, 1979), but the final R values from the structure refinement were unsatisfactory. Subsequent single-crystal X-ray structure analyses gave acceptable R values, but contradictory results, *e.g.* Ebner & Thompson (1991) reported space group $Pca2_1$ with disorder on the V sites, while Nguyen *et al.* (1995) found space group $P112_1$ with a pseudo-orthorhombic translation lattice, as indicated by a monoclinic angle of $89.975(3)^\circ$. The $P112_1$ structure model seems to be doubtful, since it presents extremely distorted non-positive definite thermal vibration ellipsoids for several V and P sites, but also unusually large isotropic displacement parameters for two O sites that are shared by opposing PO_4 tetrahedra in the P_2O_7 groups. Recent diffraction studies with X-rays, neutrons and electrons on $(\text{VO})_2\text{P}_2\text{O}_7$ powder samples showed systematic extinctions which are consistent with space group $Pca2_1$, and led to a structure model with exceptionally large isotropic displacement parameters for a number of O sites in the P_2O_7 groups also (Hiroi *et al.*, 1999). Crystallographic disorder in $(\text{VO})_2\text{P}_2\text{O}_7$ was often detected in X-ray and electron-diffraction patterns as diffuse scattering (Bordes & Courtine, 1979; Hiroi *et al.*, 1999) and peak-broadening effects due to the introduction of stacking faults (Nguyen *et al.*, 1996). Several studies revealed the ability of $(\text{VO})_2\text{P}_2\text{O}_7$ to accommodate various disordered or polytypic structures generated by interlayer vacancies (Thompson *et al.*, 1994) and O defect sites (Gai & Kourtakis, 1995; Gai, 1997). On the other hand, the

structure of $(\text{VO})_2\text{P}_2\text{O}_7$ is capable of preserving mixed-valence $\text{V}^{4+}/\text{V}^{5+}$ pairs associated with interstitial O sites in the P_2O_7 sublattice (López-Granados *et al.*, 1993). Very recently, a high-pressure phase treated at 2–3 GPa was found to crystallize in the orthorhombic space group $Pnab$, with a unit cell of half the size of that of the ambient-pressure phase (Azuma *et al.*, 1999; Saito *et al.*, 2000).

Our investigations were motivated by the fact that none of the previously published crystal structure data of the ambient-pressure phase of $(\text{VO})_2\text{P}_2\text{O}_7$ provide accurate enough values for the spin-orbital interaction energies (Koo & Whangbo, 2000). Knowledge of these spin-orbital interaction energies is indispensable to conclude unambiguously which of the alternating spin chains has the larger energy gap, and which of the bridged and edge-sharing spin dimers has the stronger spin exchange interaction in the chains. The complications in earlier studies may be attributed to sample preparation conditions, poor crystal quality, and limited experimental accuracy. The present structure determination from low-temperature synchrotron X-ray data measured on a high-quality single crystal confirms the assignment of space group $Pca2_1$. Moreover, the structure refinement provides reliable anisotropic displacement parameters for all atoms, and improves the accuracy of the atomic coordinates, as given by Hiroi *et al.* (1999) and Gorbunova & Linde (1979), by one order of magnitude.

The asymmetric unit of $(\text{VO})_2\text{P}_2\text{O}_7$ in $Pca2_1$ contains four V sites, four P sites and 18 O sites. Along the a axis, the crystal structure consists of infinite two-leg ladders of vanadyl cations, $(\text{VO})^{2+}$, which are separated by pyrophosphate anions,

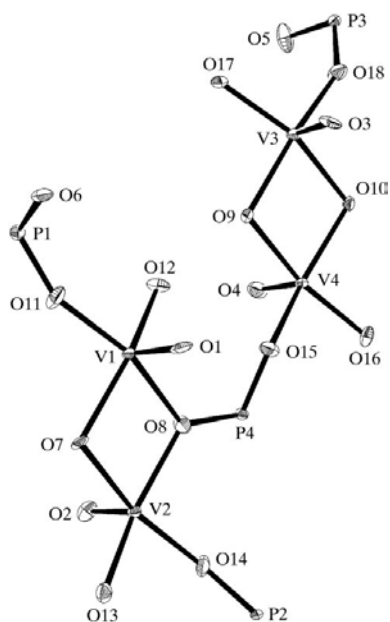


Figure 1
Polyhedral representation of the crystal structure of $(\text{VO})_2\text{P}_2\text{O}_7$ viewed (a) along the $[100]$ direction and (b) along the $[010]$ direction. The VO_5 square pyramids are drawn in dark grey, the PO_4 tetrahedra in light grey. Large circles represent V atoms and medium circles represent P atoms. Small circles in (a) denote O atoms, which are not shown in (b).

$(\text{P}_2\text{O}_7)^{4-}$. All V atoms show a (4+1) square-pyramidal coordination to five O atoms, consisting of four equatorial V–O distances ranging from 1.940 (3) to 2.083 (4) Å and one short axial V–O distance varying between 1.594 (3) and 1.612 (4) Å. In the $[100]$ direction and nearly opposite the strong $\text{V}=\text{O}$ bond of the vanadyl group, the V atoms are also weakly coordinated to the apical O atoms of neighbouring VO_5 pyramids, with long V–O distances ranging from 2.250 (4) to 2.341 (3) Å. Along the c axis, the unit cell of $(\text{VO})_2\text{P}_2\text{O}_7$ comprises two alternating crystallographically inequivalent chains built of pairs of edge-sharing VO_5 square pyramids. The chains are arranged in such a way that in every VO_5 pair the $\text{V}=\text{O}$ bonds are in *trans* positions, as each axial O atom is located alternately above or below the basal plane. The VO_5 double pyramids in the V1–V2 chain are bridged by tilted PO_4 double tetrahedra involving P1 and P2 [with a $\text{P1}\cdots\text{P2}$ separation of 3.0112 (18) Å], while those in the V3–V4 chain are linked by untilted PO_4 double tetrahedra involving P3 and P4 [with a $\text{P3}\cdots\text{P4}$ separation of 3.0873 (19) Å]. Each equatorial O atom of the VO_5 pairs shares a corner with one PO_4 group (Fig. 1). The P–O distances range from 1.487 (4) to 1.583 (3) Å and the O–P–O bond angles within the PO_4 tetrahedra vary between 104.1 (2) and 116.9 (2)°. The P1–O6–P2 and P3–O5–P4 bridging angles are 144.50 (18) and 157.20 (17)°, respectively. Both values fall within the typical range found for P_2O_7 groups. The shortest non-bonding $\text{V}\cdots\text{V}$ distances in the $[001]$

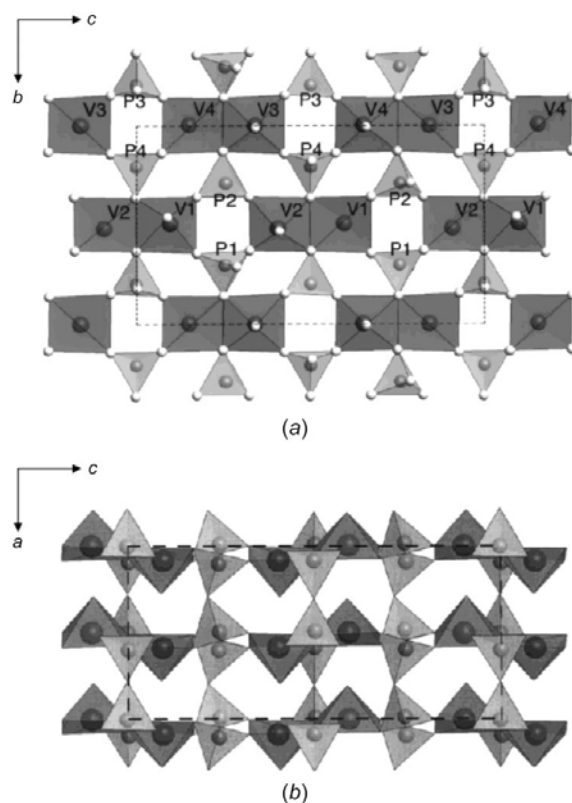


Figure 2
View of $(\text{VO})_2\text{P}_2\text{O}_7$ with the atom-labelling scheme. Displacement ellipsoids at 120 K are drawn at the 90% probability level.

direction (*i.e.* along the rungs of the ladder) are $d(V3 \cdots V4) = 3.2047$ (12) Å and $d(V1 \cdots V2) = 3.2282$ (12) Å. Those in the [100] direction (*i.e.* along the legs of the ladder) are much longer and approximately given as $a/2 = 3.85$ Å. Bond-valence calculations were carried out with the program *VALENCE* (Brown, 1996), using bond-valence parameters according to Brese & O'Keeffe (1991). The bond-valence sums agree very well with the expected valence states V^{4+} and P^{5+} (Table 2), and exclude the presence of mixed-valence V^{4+}/V^{5+} pairs for the measured crystal. The equivalent isotropic displacement parameters of the O atoms are found to be significantly larger than those of the V and P atoms, and the principal mean-square atomic displacements of several O sites show a pronounced anisotropy (Fig. 2). The thermal motion of these O atoms could not be reasonably well described by a split-atom model.

At $T = 300$ K, the lattice parameters of $(VO)_2P_2O_7$ have been determined as $a = 7.7285$ (3), $b = 9.5842$ (4) and $c = 16.5962$ (6) Å. Assuming a simple linear behaviour, the coefficients of linear thermal expansion in the temperature range between 300 and 120 K are estimated as $\alpha_a = 2.0 \times 10^{-5} K^{-1}$, $\alpha_b = 3.8 \times 10^{-6} K^{-1}$ and $\alpha_c = 4.6 \times 10^{-6} K^{-1}$. This indicates a strong anisotropic thermal expansion, taking place mainly in the direction parallel to the legs of the ladder. The α value is comparable with that obtained from Raman scattering experiments (Kuhlmann *et al.*, 2001).

Experimental

In general, the single-crystal growth of $(VO)_2P_2O_7$ is complicated by two features. First, the phase stability and valence state of vanadium are very sensitive to the oxygen content in the growth atmosphere (López-Granados *et al.*, 1993; Prokofiev *et al.*, 2000). Secondly, the melt exhibits a tendency towards glass formation during cooling due to its high viscosity. Therefore, the single-crystal growth has to be carried out with a very low growth rate and in a growth atmosphere with controlled oxygen content. $(VO)_2P_2O_7$ powder for the crystal growth was prepared from the precursor vanadyl hydrogen phosphate hemihydrate, $VOHPO_4 \cdot 0.5H_2O$, via a topotactic dehydration (Bordes *et al.*, 1984; Torardi *et al.*, 1995) in an argon flow at 973 K. The precursor was synthesized according to the procedure given by Centi *et al.* (1985). Large single crystals of $(VO)_2P_2O_7$ were grown using a combination of Czochralski and Kryopoulos methods, *i.e.* slow cooling (4–8 K per day) of the melt with simultaneous pulling (2 mm per day) of the dark-green crystals from the melt. Crystal growth was carried out in a resistance furnace under a flow of a gas mixture of argon and oxygen (0.2 vol%), using a silica growth chamber and a platinum crucible. Further details of the crystal-growth technique are described by Prokofiev, Büllersfeld & Assmus (1998). No impurity phases were detected using electron microprobe analysis, scanning electron microscopy, and X-ray powder diffraction. From thermogravimetric analysis studies based on the oxidation of $(VO)_2P_2O_7$ to VPO_5 , the oxidation state of the V ions was determined to be +4.05. Furthermore, the single crystals were comprehensively investigated using electron spin resonance and magnetic susceptibility measurements (Prokofiev, Büllersfeld, Assmus *et al.*, 1998), as well as Raman scattering and IR spectroscopy (Kuhlmann *et al.*, 2000, 2001; Grove *et al.*, 2000).

Crystal data

$(VO)_2P_2O_7$
 $M_r = 307.82$
 Orthorhombic, $Pca2_1$
 $a = 7.7004$ (4) Å
 $b = 9.5777$ (5) Å
 $c = 16.5825$ (8) Å
 $V = 1222.99$ (11) Å³
 $Z = 8$
 $D_x = 3.344$ Mg m⁻³

Synchrotron radiation
 $\lambda = 0.70843$ Å
 Cell parameters from 25 reflections
 $\theta = 16.1$ – 22.5°
 $\mu = 3.55$ mm⁻¹
 $T = 120$ (2) K
 Rectangular prism, dark green
 $0.10 \times 0.04 \times 0.03$ mm

Data collection

Huber four-circle Kappa diffractometer with a Siemens SMART CCD area-detector and an Oxford Cryosystems Cryostream cooler
 ω and φ scans
 Absorption correction: multi-scan (*SADABS*; Sheldrick, 1996)
 $T_{\min} = 0.804$, $T_{\max} = 0.950$

11 910 measured reflections
 3149 independent reflections
 2452 reflections with $I > 2\sigma(I)$
 $R_{\text{int}} = 0.060$
 $\theta_{\text{max}} = 30.4^\circ$
 $h = -10 \rightarrow 9$
 $k = -13 \rightarrow 13$
 $l = -23 \rightarrow 23$

Refinement

Refinement on F^2
 $R[F^2 > 2\sigma(F^2)] = 0.031$
 $wR(F^2) = 0.068$
 $S = 0.88$
 3149 reflections
 237 parameters
 $w = 1/[\sigma^2(F_o^2) + (0.0302P)^2]$
 where $P = (F_o^2 + 2F_c^2)/3$
 $(\Delta/\sigma)_{\text{max}} < 0.001$

$\Delta\rho_{\text{max}} = 0.81$ e Å⁻³
 $\Delta\rho_{\text{min}} = -0.67$ e Å⁻³
 Extinction correction: *SHELXL97* (Sheldrick, 1997)
 Extinction coefficient: 0.0165 (6)
 Absolute structure: Flack (1983), 1303 Friedel pairs
 Flack parameter = 0.00 (13)

Table 1
 Selected geometric parameters (Å, °).

V1–O1	1.594 (3)	V4–O15 ^{vii}	1.942 (3)
V1–O11 ⁱ	1.941 (3)	V4–O9 ^{viii}	2.050 (4)
V1–O12	1.949 (3)	V4–O10	2.073 (4)
V1–O7 ⁱ	2.079 (4)	V4–O4	2.250 (4)
V1–O8	2.083 (4)	P1–O11	1.487 (4)
V1–O1 ⁱⁱ	2.341 (3)	P1–O13 ^{vii}	1.499 (4)
V2–O2	1.600 (5)	P1–O10	1.557 (4)
V2–O14 ⁱⁱⁱ	1.951 (4)	P1–O6 ^{ix}	1.583 (3)
V2–O13	1.957 (4)	P2–O12	1.490 (3)
V2–O8 ^{iv}	2.071 (4)	P2–O14	1.498 (4)
V2–O7	2.071 (4)	P2–O9	1.556 (3)
V2–O2 ^v	2.305 (5)	P2–O6	1.579 (3)
V3–O3 ^{vi}	1.603 (6)	P3–O18	1.487 (4)
V3–O17 ^{vii}	1.944 (4)	P3–O16	1.494 (3)
V3–O18	1.954 (4)	P3–O7	1.554 (3)
V3–O9	2.070 (4)	P3–O5 ^{ix}	1.576 (3)
V3–O10 ^{viii}	2.077 (4)	P4–O15	1.495 (4)
V3–O3	2.256 (6)	P4–O17	1.498 (4)
V4–O4 ^{vi}	1.612 (4)	P4–O8	1.554 (3)
V4–O16	1.940 (3)	P4–O5	1.573 (3)
P4–O5–P3 ^x	157.20 (17)	P2–O6–P1 ^x	144.50 (18)

Symmetry codes: (i) $\frac{1}{2} - x, y - 1, \frac{1}{2} + z$; (ii) $\frac{1}{2} + x, -y, z$; (iii) $x, 1 + y, z$; (iv) $\frac{1}{2} - x, 1 + y, z - \frac{1}{2}$; (v) $\frac{1}{2} + x, 2 - y, z$; (vi) $x - \frac{1}{2}, 1 - y, z$; (vii) $\frac{1}{2} - x, y, z - \frac{1}{2}$; (viii) $\frac{1}{2} - x, y, \frac{1}{2} + z$; (ix) $1 - x, 1 - y, z - \frac{1}{2}$; (x) $1 - x, 1 - y, \frac{1}{2} + z$.

Table 2
 Selected bond-valence sums.

Atom	Bond-valence sum	Atom	Bond-valence sum
V1	4.08	P1	4.89
V2	4.07	P2	4.90
V3	4.11	P3	4.94
V4	4.13	P4	4.91

Table 3
Bond-valence data.

Atom 1	Valence	Atom 2	Valence	R_o	B	Ref.
V	4	O	-2	1.784	0.370	(a)
P	5	O	-2	1.604	0.370	(a)

Notes: (a) Brese & O'Keeffe (1991).

Single-crystal X-ray diffraction experiments with synchrotron radiation were performed on beamline F1 of HASYLAB at DESY Hamburg. A double-crystal Si(111) monochromator was used to select a wavelength of $\lambda = 0.70843 \text{ \AA}$. Reflection groups $h0l$ ($h = 2n + 1$), $0kl$ ($l = 2n + 1$), $h00$ ($h = 2n + 1$) and $00l$ ($l = 2n + 1$) were found to be systematically absent in the data collection carried out at $T = 120 \text{ K}$, with a measuring time of 5 s per frame and a crystal-to-detector distance of 50 mm. Possible space groups consistent with the observed reflection conditions are only $Pcam$ or $Pca2_1$. Indications of disorder, non-merohedral twinning or superstructure reflections were not detected. *SADABS* (Sheldrick, 1996) was used for corrections of variations in the primary beam intensity and for averaging symmetry-equivalent reflections. Accurate lattice parameters at 120 and 300 K were determined from laboratory four-circle diffractometer data, because several systematic errors (e.g. the positions of the crystal and detector) in the cell-refinement procedure are not accounted for by *SAINT* (Siemens, 1996). We checked the monoclinic cell constraints also, but none of the unit-cell angles differed from 90° within one standard deviation.

The Flack (1983) parameter of an initial refinement in space group $Pca2_1$ indicated that the crystal was twinned. The refinement model without twinning yielded a Flack parameter of $x = 0.27$ (4), with $R = 0.0308$ and $wR = 0.0692$. Transformation to the inverse structure resulted in $x = 0.54$ (4), with $R = 0.0316$ and $wR = 0.0716$. Consequently, an inversion twin was added to the structure model. The final refinement gave a twin volume fraction of 34 (4)%. This value is in good agreement with a ratio of 32% determined with the program *TWIN3.0* (Kahlenberg & Messner, 2000), using the procedure proposed by Britton (1972). The deviation from the expected 1:1 distribution may be caused during the cutting of the crystals. Fixing the twin fraction at 50% had no significant influence on the structure parameters.

Due to the facts that all V atoms are located very close to $y = 0$ or $y = \frac{1}{2}$ and that such pairs of related atoms in $Pca2_1$ do not contribute to the intensities of reflections with $h = 2n + 1$ (Marsh *et al.*, 1998), almost all $hk0$ reflections with $h = 2n + 1$ were also found to be absent in the data collection [average $I/\sigma(I) = 1.3$ and maximum $I/\sigma(I) = 10$]. This suggests the centrosymmetric space group $Pcaa$, which is a translationengleiche supergroup of index 2 of $Pca2_1$. The possible existence of an a -glide plane perpendicular to the c axis as an additional pseudosymmetry element (with 20% non-fitting atoms) was detected by *PLATON* (Spek, 2001) also. When the match tolerance for pseudo-translations was reduced to 0.1 Å, the extra symmetry disappeared. Although several pairs of unique atoms in the $Pca2_1$ model seem to be related by an additional a -glide plane perpendicular to the c axis, five unique atoms (V3, V4, P1, P2 and O6) have no symmetry-related counterpart. Therefore, this a -glide plane may represent a pseudosymmetry element rather than a true crystallographic one. Even though the structure could be solved in $Pcaa$ (26 systematic absence violations, $R_{\text{int}} = 0.063$ for 1792 independent reflections) with direct methods, the refined structure model involving split-atom positions remains deficient ($R = 0.129$ for 142 para-

eters and 1443 observed reflections), and unacceptably high residuals (3.6 and -6.4 e \AA^{-3}) lying close to the V atoms appear in the difference Fourier map. Attempts to refine the data in $Pcam$ ($R_{\text{int}} = 0.063$ for 1848 independent reflections) were also unsuccessful ($R = 0.121$ for 151 parameters and 1466 observed reflections, highest residuals 2.9 and -5.3 e \AA^{-3}), although the statistical distribution of normalized structure factors strongly prefers a centrosymmetric space group (the values of $|E^2 - 1|$ are 1.273 for $0kl$, 1.040 for $h0l$, 1.076 for $hk0$, and 0.947 for all other reflections). Assuming monoclinic symmetry with space group $P112_1$ (inversion twin, $R_{\text{int}} = 0.057$ for 5581 independent reflections), the final R values are, in comparison with those for $Pca2_1$, only slightly higher ($R = 0.0330$, $wR = 0.0758$ for 471 parameters and 3882 observed reflections, highest residuals 0.79 and -0.77 e \AA^{-3}). However, the anisotropic displacement parameters of five unique O atoms in $P112_1$ possess a principal axis $U_{\text{max}}/U_{\text{min}}$ ratio of more than 15:1, and the anisotropic displacement ellipsoids of three further O atoms even become non-positive definite, while those of all the atoms in $Pca2_1$ display a physically meaningful shape.

Data collection: *SMART* (Siemens, 1996); cell refinement: *SET4* in *CAD-4 UNIX Software* (Enraf-Nonius, 1998); data reduction: *SAINT* (Siemens, 1996); program(s) used to solve structure: *SHELXS97* (Sheldrick, 1997); program(s) used to refine structure: *SHELXL97* (Sheldrick, 1997); molecular graphics: *DIAMOND* (Brandenburg, 1999) and *ORTEP-3* (Farrugia, 1997); software used to prepare material for publication: *SHELXL97*.

The authors thank H. Schmidt and H.-G. Krane for experimental support on HASYLAB. Financial support from the Deutsche Forschungsgemeinschaft (DFG) is gratefully acknowledged.

Supplementary data for this paper are available from the IUCr electronic archives (Reference: BR1349). Services for accessing these data are described at the back of the journal.

References

- Azuma, M., Saito, T., Fujishiro, Y., Hiroi, Z., Takano, M., Izumi, F., Kamiyama, T., Ikeda, T., Narumi, Y. & Kindo, K. (1999). *Phys. Rev. B*, **60**, 10145–10149.
- Barnes, T., Dagotto, E., Riera, J. & Swanson, E. S. (1993). *Phys. Rev. B*, **47**, 3196–3203.
- Barnes, T. & Riera, J. (1994). *Phys. Rev. B*, **50**, 6817–6822.
- Bordes, E. & Courtine, P. (1979). *J. Catal.* **57**, 236–252.
- Bordes, E., Courtine, P. & Johnson, J. W. (1984). *J. Solid State Chem.* **55**, 270–279.
- Brandenburg, K. (1999). *DIAMOND*. Version 2.1c. Crystal Impact GbR, Bonn, Germany.
- Brese, N. E. & O'Keeffe, M. (1991). *Acta Cryst.* **B47**, 192–197.
- Britton, D. (1972). *Acta Cryst.* **A28**, 296–297.
- Brown, I. D. (1996). *J. Appl. Cryst.* **29**, 479–480.
- Centi, G., Trifirò, F., Ebner, J. R. & Franchetti, V. M. (1988). *Chem. Rev.* **88**, 55–80.
- Centi, G., Trifirò, F. & Poli, G. (1985). *Appl. Catal.* **19**, 225–239.
- Dagotto, E. & Rice, T. M. (1996). *Science*, **271**, 618–623.
- Dagotto, E., Riera, J. & Scalapino, D. (1992). *Phys. Rev. B*, **45**, 5744–5747.
- Ebner, J. R. & Thompson, M. R. (1991). *Studies in Surface Science and Catalysis*, Vol. 68, edited by R. K. Grasselli & A. W. Sleight, pp. 31–42. Amsterdam: Elsevier.
- Eccleston, R. S., Barnes, T., Brody, J. & Johnson, J. W. (1994). *Phys. Rev. Lett.* **73**, 2626–2629.
- Enraf-Nonius (1998). *CAD-4 UNIX Software*. Utrecht modified version 5.1. Enraf-Nonius, Delft, The Netherlands.
- Farrugia, L. J. (1997). *J. Appl. Cryst.* **30**, 565.

- Flack, H. D. (1983). *Acta Cryst.* **A39**, 876–881.
- Gai, P. L. (1997). *Acta Cryst.* **B53**, 346–352.
- Gai, P. L. & Kourtakis, K. (1995). *Science*, **267**, 661–663.
- Garrett, A. W., Nagler, S. E., Barnes, T. & Sales, B. C. (1997). *Phys. Rev. B*, **55**, 3631–3635.
- Garrett, A. W., Nagler, S. E., Tennant, D. A., Sales, B. C. & Barnes, T. (1997). *Phys. Rev. Lett.* **79**, 745–748.
- Gorbunova, Yu. E. & Linde, S. A. (1979). *Sov. Phys. Dokl.* **24**, 138–140.
- Grove, M., Lemmens, P., Güntherodt, G., Sales, B. C., Büllersfeld, F. & Assmus, W. (2000). *Phys. Rev. B*, **61**, 6126–6132.
- Hiroi, Z., Azuma, M., Fujishiro, Y., Saito, T., Takano, M., Izumi, F., Kamiyama, T. & Ikeda, T. (1999). *J. Solid State Chem.* **146**, 369–379.
- Johnston, D. C., Johnson, J. W., Goshorn, D. P. & Jacobson, A. J. (1987). *Phys. Rev. B*, **35**, 219–222.
- Johnston, D. C., Saito, T., Azuma, M., Takano, M., Yamauchi, T. & Ueda, Y. (2001). *Phys. Rev. B*, **64**, 134403.
- Kahlenberg, V. & Messner, T. (2000). *TWIN3.0*. University of Bremen, Germany.
- Kikuchi, J., Motoya, K., Yamauchi, T. & Ueda, Y. (1999). *Phys. Rev. B*, **60**, 6731–6739.
- Koo, H.-J. & Whangbo, M.-H. (2000). *Inorg. Chem.* **39**, 3599–3604.
- Kuhlmann, U., Thomsen, C., Prokofiev, A. V., Büllersfeld, F., Uhrig, E. & Assmus, W. (2000). *Phys. Rev. B*, **62**, 12262.
- Kuhlmann, U., Thomsen, C., Prokofiev, A. V., Büllersfeld, F., Uhrig, E. & Assmus, W. (2001). *Physica B*, **301**, 276–285.
- López-Granados, M., Conesa, J. C. & Fernández-García, M. (1993). *J. Catal.* **141**, 671–687.
- Marsh, R. E., Schomaker, V. & Herbstein, F. H. (1998). *Acta Cryst.* **B54**, 921–924.
- Nguyen, P. T., Hoffman, R. D. & Sleight, A. W. (1995). *Mater. Res. Bull.* **30**, 1055–1063.
- Nguyen, P. T., Sleight, A. W., Roberts, N. & Warren, W. W. (1996). *J. Solid State Chem.* **122**, 259–265.
- Prokofiev, A. V., Büllersfeld, F. & Assmus, W. (1998). *Cryst. Res. Technol.* **33**, 157–163.
- Prokofiev, A. V., Büllersfeld, F. & Assmus, W. (2000). *Mater. Res. Bull.* **35**, 1859–1868.
- Prokofiev, A. V., Büllersfeld, F., Assmus, W., Schwenk, H., Wichert, D., Löw, U. & Lüthi, B. (1998). *Eur. Phys. J.* **B5**, 313–316.
- Saito, T., Terashima, T., Azuma, M., Takano, M., Goto, T., Ohta, H., Utsumi, W., Bordet, P. & Johnston, D. C. (2000). *J. Solid State Chem.* **153**, 124–131.
- Sheldrick, G. M. (1996). *SADABS*. University of Göttingen, Germany.
- Sheldrick, G. M. (1997). *SHELXS97* and *SHELXL97*. University of Göttingen, Germany.
- Siemens (1996). *SMART* and *SAINT*. Siemens Analytical X-ray Instruments Inc., Madison, Wisconsin, USA.
- Spek, A. L. (2001). *PLATON*. Utrecht University, The Netherlands.
- Thompson, M. R., Hess, A. C., Nicholas, J. B., White, J. C., Anchell, J. & Ebner, J. R. (1994). *Studies in Surface Science and Catalysis*, Vol. 82, edited by V. C. Corberan & S. V. Bellon, p. 167. Amsterdam: Elsevier.
- Torardi, C. C., Li, Z. G., Horowitz, H. S., Liang, W. & Whangbo, M.-H. (1995). *J. Solid State Chem.* **119**, 349–358.
- Yamauchi, T., Narumi, Y., Kikuchi, J., Ueda, Y., Tatani, K., Kobayashi, T. C., Kindo, K. & Motoya, K. (1999). *Phys. Rev. Lett.* **83**, 3729–3732.

Synchrotron-radiation study of the two-leg spin ladder $(VO)_2P_2O_7$ at 120 K. Erratum

Sandra Geupel,^{a*} Katrin Pilz,^a Sander van Smaalen,^a Frank
Büllesfeld,^b Andrei Prokofiev^b and Wolf Assmus^b

^aLaboratory of Crystallography, University of Bayreuth, D-95440 Bayreuth,
Germany, and ^bInstitute of Physics, University of Frankfurt, D-60054 Frankfurt am
Main, Germany

Correspondence e-mail: sandra.geupel@uni-bayreuth.de

Two errors in the paper by Geupel *et al.* [*Acta Cryst.* (2002), C58, i9–i13] are reported. The figures on page i10 are printed in the wrong order, *i.e.* Fig. 1 should in fact be Fig. 2 and *vice versa*. The figure captions are given correctly. In the last sentence of the *Comment* section, the coefficient α of the linear thermal expansion should be replaced by α_a (with the subscript referring to the *a* axis of the orthorhombic unit cell), so that the sentence reads ‘The α_a value is comparable with that obtained from Raman scattering experiments....’.

References

Geupel, S., Pilz, K., van Smaalen, S., Prokofiev, A. V., Büllesfeld, F. & Assmus, W. (2002). *Acta Cryst.* C58, i9–i13.